

# Nuclear localization of barrier-to-autointegration factor is correlated with progression of S phase in human cells

Tokuko Haraguchi<sup>1,2,\*</sup>, Takako Koujin<sup>1</sup>, Hiroko Osakada<sup>1</sup>, Tomoko Kojidani<sup>1</sup>, Chie Mori<sup>1</sup>, Hirohisa Masuda<sup>1</sup> and Yasushi Hiraoka<sup>1,2</sup>

<sup>1</sup>CREST Research Project, Kansai Advanced Research Center, National Institute of Information and Communications Technology, 588-2 Iwaoka, Iwaoka-cho, Nishi-ku, Kobe 651-2492, Japan

<sup>2</sup>Graduate School of Science, Osaka University, 1-1 Machikaneyama, Toyonaka 560-0043, Osaka, Japan

\*Author for correspondence (e-mail: tokuko@nict.go.jp)

Accepted 19 April 2007

Journal of Cell Science 120, 1967-1977 Published by The Company of Biologists 2007  
doi:10.1242/jcs.03461

## Summary

Barrier-to-autointegration factor (BAF) is a conserved metazoan protein that plays a critical role in retrovirus infection. To elucidate its role in uninfected cells, we first examined the localization of BAF in both mortal and immortal or cancerous human cell lines. In mortal cell lines (e.g. TIG-1, WI-38 and IMR-90 cells) BAF localization depended on the age of the cell, localizing primarily in the nucleus of >90% of young proliferating cells but only 20-25% of aged senescent cells. In immortal cell lines (e.g. HeLa, SiHa and HT1080 cells) BAF showed heterogeneous localization between the nucleus and cytoplasm. This heterogeneity was lost when the cells were synchronized in S phase. In S-phase-synchronized populations, the percentage of cells with predominantly nuclear BAF increased from 30% (asynchronous controls) to ~80%. In

HeLa cells, RNAi-induced downregulation of BAF significantly increased the proportion of early S-phase cells that retained high levels of cyclin D3 and cyclin E expression and slowed progression through early S phase. BAF downregulation also caused lamin A to mislocalize away from the nuclear envelope. These results indicate that BAF is required for the integrity of the nuclear lamina and normal progression of S phase in human cells.

Supplementary material available online at  
<http://jcs.biologists.org/cgi/content/full/120/12/1967/DC1>

Key words: BAF, Nuclear envelope, Chromatin, Emerin, Lamin A, Aging

## Introduction

Barrier-to-autointegration factor (BAF), a ~10 kDa dsDNA-binding protein, was first discovered as a host component of retroviral pre-integration complexes that facilitated integrase-mediated integration into target DNA in vitro (Lee and Craigie, 1994) (reviewed by Segura-Totten and Wilson, 2004). BAF was recently shown to be essential for HIV-1 infection of macrophages in vivo (Jacque and Stevenson, 2006). BAF exists as a dimer in solution (Cai et al., 1998) and binds dsDNA in vitro in a sequence-non-specific manner through a helix-hairpin-helix motif common to other DNA-binding proteins (Zheng et al., 2000; Umland et al., 2000; Bradley et al., 2005). BAF does not bind single-stranded DNA or RNA. Curiously, in the presence of 21-bp dsDNA, BAF dimers can associate as hexamers of dimers in vitro (Zheng et al., 2000). This activity is exploited by retroviruses to compact the retroviral DNA prior to integration (Zheng et al., 2000), but whether BAF has similar activity in uninfected cells remains unknown.

BAF is highly conserved among metazoans (Lee and Craigie, 1998) and has many conserved interacting partners. One group of partners comprises the entire LEM-domain family of nuclear proteins (Furukawa, 1999; Shumaker et al., 2001). This family was named for founding members lamina-associated polypeptide 2 (LAP2), emerin and MAN1, which

share a ~40-residue folded LEM domain (Lin et al., 2000). The human genome encodes at least four additional LEM-domain proteins, including LEM2 (Lee and Wilson, 2004; Schirmer et al., 2003; Brachner et al., 2005). The diversity of LEM-domain proteins is increased by alternative splicing of the LAP2 gene, found only in vertebrates, which generates six isoforms (Dechat et al., 2000). Among them, LAP2 $\beta$  has a C-terminal transmembrane domain and localizes at the nuclear inner membrane. By contrast, LAP2 $\alpha$ , which has no transmembrane domain, is a mobile protein in the nuclear interior (Dechat et al., 2004). Interestingly, during mitosis, LAP2 $\alpha$  forms a stable complex with BAF that targets telomeres (Dechat et al., 2004). LAP2 $\alpha$  also appears to form a stable complex with BAF in retroviral pre-integration complexes (Suzuki et al., 2004). All characterized LEM-domain proteins bind lamins (A- or B-type, or both). Most (including emerin and MAN1) are integral membrane proteins that colocalize with the lamina network at the inner nuclear membrane, but some (e.g. LAP2 $\alpha$ ) associate with lamin complexes in the nuclear interior (Foisner, 2001). In addition to LEM-domain proteins, BAF also binds directly to lamin A (Holaska et al., 2003), a BAF-related protein named BAF-L (Tiffet et al., 2006), homeodomain transcription activators including Crx (Wang et al., 2002), histone H3 and selected linker histones including histone H1.1 (Montes de Oca

et al., 2005). Based on these partners and the demonstrated effects of BAF on higher-order chromatin structure, BAF is proposed to influence chromatin structure through mechanisms that are currently unknown, and to help anchor chromatin to the nuclear inner membrane (Segura-Totten and Wilson, 2004).

BAF function has been studied in several systems. BAF is essential for embryogenesis in *Caenorhabditis elegans* (Zheng et al., 2000; Margalit et al., 2005) and localizes in the nucleus with enrichment at the nuclear envelope. Experiments in which BAF was downregulated by RNA interference showed that BAF is required during mitosis for chromosome segregation, chromosome decondensation and nuclear envelope assembly (Zheng et al., 2000; Margalit et al., 2005). In *Drosophila melanogaster* embryos and larvae, BAF also localizes predominantly in the nucleus, but specifically colocalizes with chromatin (Furukawa et al., 2003). In fly embryos that are homozygous-null for the *BAF* gene, maternally supplied BAF protein was sufficient for survival through embryogenesis; however, when BAF was ultimately depleted in the late larval stage, cells developed gross abnormalities in interphase nuclear shape, aberrant chromosome organization and abnormal distribution of lamin B, and apparently arrested at multiple stages of the cell cycle, possibly owing to a lack of cyclin gene expression (Furukawa et al., 2003).

One important question is where, precisely, BAF localizes in cells, because reports have differed between animal classes, and even between mammalian species. In rat FRSK cells, BAF localized predominantly in the nucleus during interphase and on chromosomes during mitosis (Furukawa, 1999), a pattern similar to *Drosophila* (Furukawa et al., 2003). On the other hand, BAF is present in both the nucleus and cytoplasm in *C. elegans* (Margalit et al., 2005) and *Xenopus* A6 cells (Segura-Totten et al., 2002), with enrichment at the nuclear envelope during interphase. Intriguingly, during telophase of mitosis, BAF is enriched in specialized ('core') regions of the chromosome mass near the spindle (Haraguchi et al., 2001). This transient core localization of BAF is needed for emerlin and lamin A to reassemble into the nuclear envelope of each daughter cell (Haraguchi et al., 2001). In addition to a role in assembling the nuclear envelope at the end of mitosis, BAF appears to stabilize the nuclear envelope localization of emerlin during interphase (Bengtsson and Wilson, 2006). However, given its many partners and its poorly understood localization in the cytoplasm of some cells, we hypothesized that BAF might have additional roles during interphase in mammalian cells. Here we demonstrate that BAF localization is cell cycle regulated during S phase and also strongly affected by the physiological status of the cell, notably whether the cell is mortal or cancerous.

## Results

### BAF localization pattern is different in various cell types

To better understand BAF localization, we used indirect immunofluorescence staining in various human cell lines using affinity-purified antibodies raised against a synthetic BAF peptide (see Materials and Methods). Fig. 1A shows a typical western blot of a protein lysate from HeLa cells and the corresponding nuclear and cytosolic fractions, probed with either unpurified serum (Fig. 1A, 'before') or the affinity-purified antibody (Fig. 1A, 'after'). The unpurified serum recognized one major band that migrated at ~11 kDa (arrow),

two minor bands that migrated at ~13 kDa (arrowhead) and ~80 kDa, and several very minor bands migrating at ~45 and 70 kDa (Fig. 1A, 'before'). The 45 and 70 kDa bands were also recognized by pre-immune serum, and therefore nonspecific (data not shown). The 11 and 13 kDa bands were lost by competition with the antigenic peptide (data not shown), suggesting these two bands were specific to BAF. We further confirmed the specificity of the affinity-purified antibodies in cells that stably expressed GFP-BAF. In a protein lysate from those cells, the affinity-purified antibodies recognized a new 40 kDa band (asterisk) corresponding to GFP-BAF in addition to the 11 and 13 kDa bands (Fig. 1A, 'after', right panel), indicating the affinity-purified antibody specifically recognized BAF. We used this affinity-purified antibody in all experiments of indirect immunofluorescence in this paper.

To localize BAF by indirect immunofluorescence in HeLa cells, we first tested different fixation conditions including formalin (methanol-denatured formaldehyde solution), formaldehyde (FA), a mixture of formaldehyde and glutaraldehyde (FA-GA), cold methanol, and trichloroacetic acid (TCA). All methods tested, except methanol, gave positive signals in both the nucleus and cytoplasm of HeLa cells, and most showed the expected changes in BAF localization during mitosis (see supplementary material Fig. S1). Although TCA fixation gave a stronger nuclear envelope signal, we selected FA-GA fixation for further study because it gave the best overall signal-to-background ratio, despite its slightly lower nuclear envelope signal. This fluorescence signal was totally abolished in the presence of the antigenic peptide (compare Fig. 1B, upper vs lower panels), indicating that staining was specific to BAF. Using the FA-GA fixation condition and affinity-purified antibodies, we then detected BAF by indirect immunofluorescence in 12 different human cell lines: three primary (mortal) cell cultures (TIG1, WI-38 and IMR-90), and nine immortal and/or cancerous cell lines (HT-1080, Hep G2, KMRC-1, KMRC-2, RERF-LC-KL, A431, SiHa, HeLa and HeLa-S3). In all three primary cell cultures, BAF localized predominantly to the nucleus in more than 90% of the cells examined (more than 300 cells) (Fig. 1C, arrows in TIG-1, WI-38 and IMR-90). In the immortal, mostly cancer-derived cell lines, BAF localization differed from cell to cell, as shown above for HeLa cells: some cells showed mostly nuclear localization (Fig. 1C, arrows), others showed mostly cytoplasmic localization (Fig. 1C, arrowheads) and yet others showed BAF evenly distributed between the nucleus and cytoplasm (Fig. 1C, asterisks). These results suggest that BAF localization may be differently regulated in mortal and immortal cell lines that possess different proliferating ability.

### Age-dependent dislocalization of nuclear BAF in mortal cells

Since BAF localization differed in mortal and immortal cell lines, we speculated that BAF localization was affected by stages of cell proliferation, such as aging and/or cell cycle stages. We first examined BAF localization in normal cells of various ages with different proliferation abilities. BAF was predominantly localized to the nucleus in young proliferating TIG-1 cells examined after 15 population doublings (PD15), but the percentage of the cell population with nuclear BAF decreased in older cells with PD47 and PD63 (Fig. 2A, left panels). Under the same conditions, antibodies against other

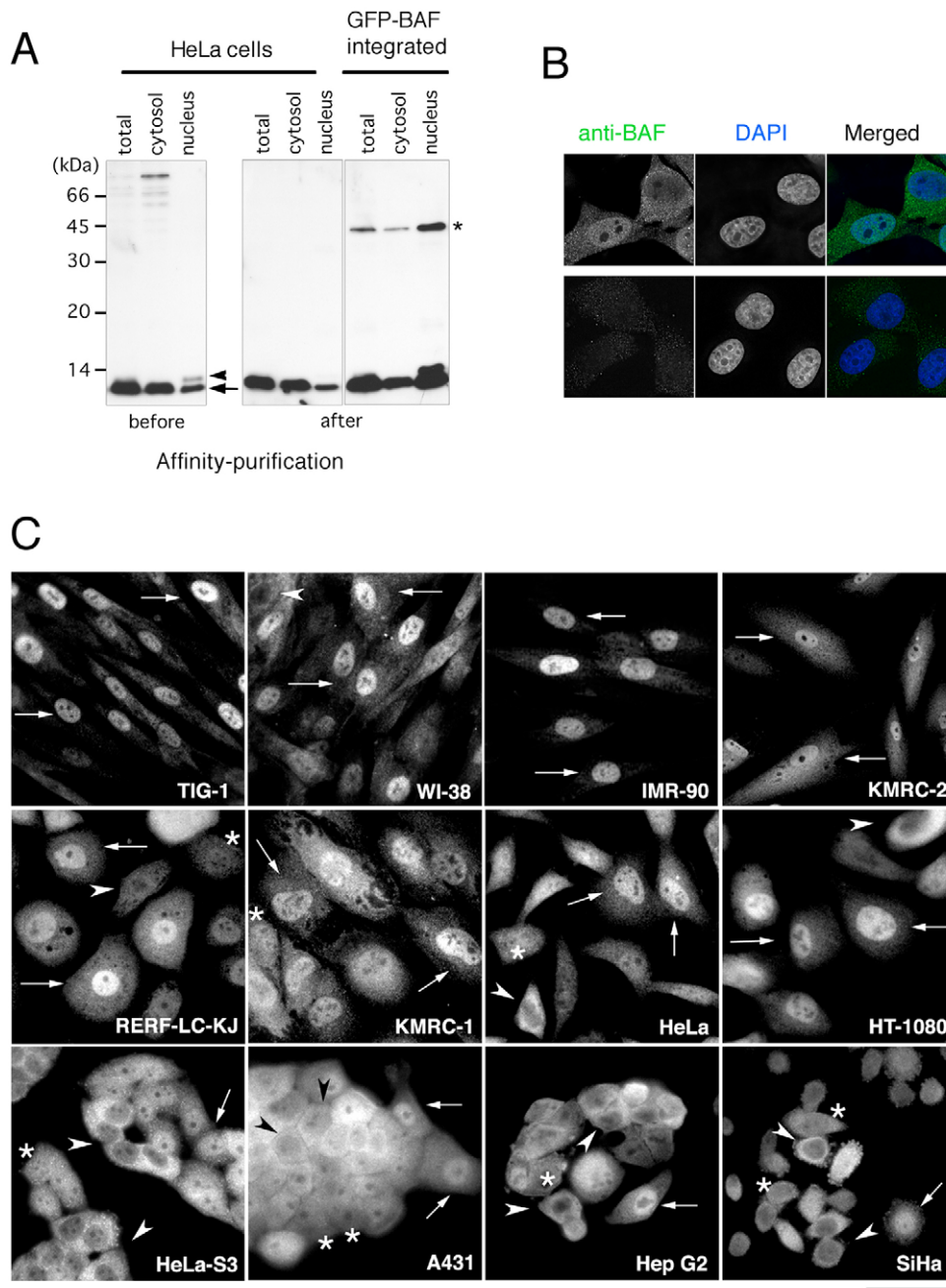


**Fig. 1.** Subcellular localization of BAF in various human cell lines.

(A) Western blotting using unpurified ('before', left panel) and affinity-purified ('after', middle and right panels) anti-BAF-3273-6 antibody. Whole extract (total), the cytoplasmic fraction (cytosol), and the nuclear fraction (nucleus) from HeLa cells (left and middle panels) and GFP-BAF-expressing HeLa cells (right panel) were analyzed. (B) Indirect immunofluorescence staining of HeLa cells using affinity-purified anti-BAF antibody (upper panels) and the same antibody pretreated with epitope peptides (lower panels). Left panels are anti-BAF staining (green in merged images), middle panels are DAPI staining for DNA (blue in merged images), and right panels are merged images. (C) Indirect immunofluorescence staining of various human cell types using affinity-purified anti-BAF antibody. Arrows represent cells with prominent nuclear signals and arrowheads represent cells with prominent cytoplasmic signals. Asterisks indicate cells with uniform signals. Bar, 40  $\mu$ m.

nuclear proteins such as lamin A and emerin stained the nucleus in aged cells, eliminating the possibility of loss of antibody accessibility in aged nuclei (data not shown). Quantitative analysis of cell populations with 'nucleus positive' (Nuc>Cyto), 'uniform' (Nuc=Cyto), and 'cytoplasm positive' (Nuc<Cyto) localization of BAF is shown for cells of PD15, PD47 and PD63 in Fig. 2B (3262 cells, 1915 cells, and 1131 cells counted, respectively). The proportion of cells with nucleus-positive BAF was high (90%) in young cells of PD15 and decreased to 42% in middle-aged cells of PD47 and to 25% in old cells of PD63. Conversely, the proportion of cytoplasm-positive cells increased from less than 1% in the young cells of PD15 to 13% in middle-aged cells of PD47 and to 43% in old cells of PD63 (compare black bars with white ones in Fig. 2B). The proportion of uniform cells also increased during

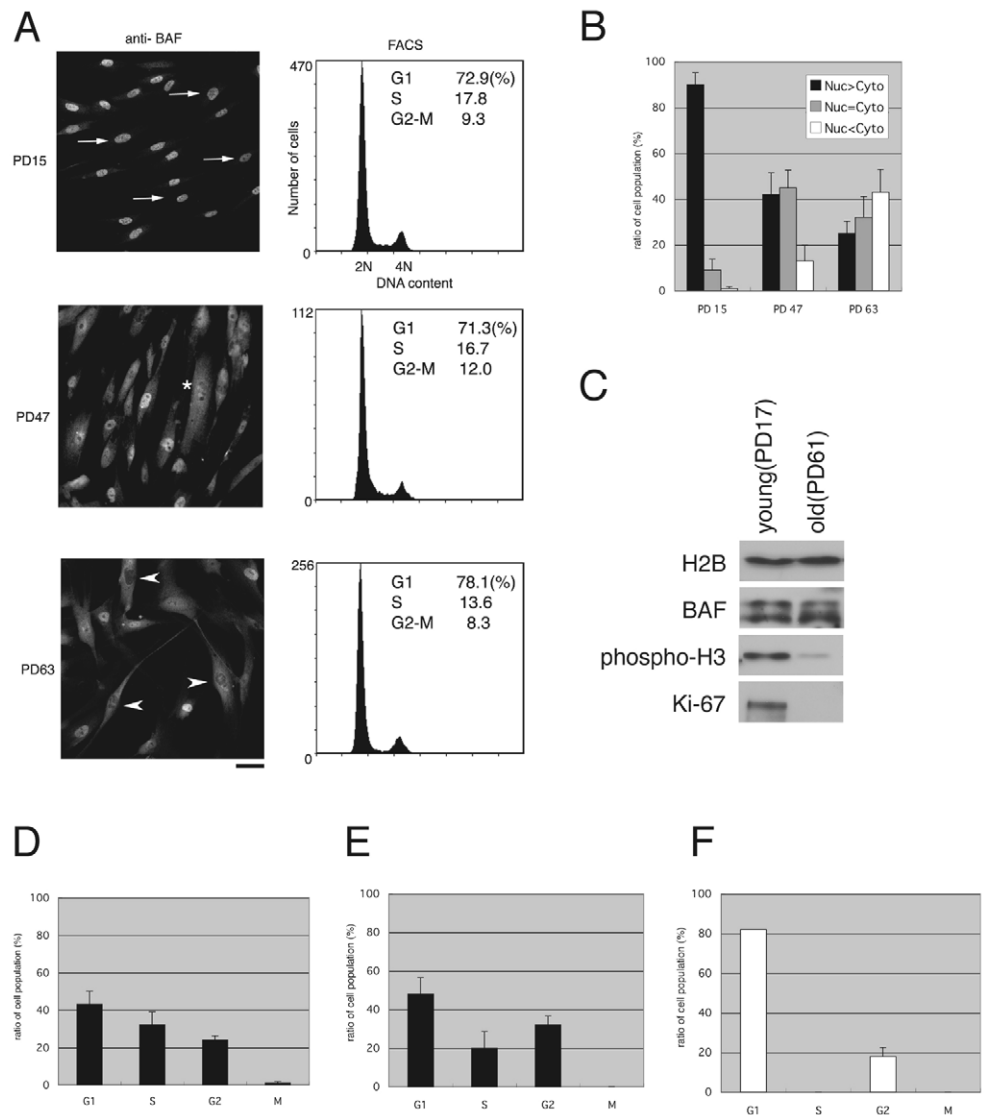
aging (see grey columns in Fig. 2B). Western blotting analysis revealed that the total amount of BAF protein did not change at all between young and old cells; compare relative BAF levels with that of histone H2B, which was used as a loading control. However, the levels of growth-marker proteins such as phosphorylated histone H3 and Ki-67 were significantly decreased in old cells as expected (Fig. 2C). This suggests that BAF protein was delocalized from the nucleus to the cytoplasm during aging, but that overall protein levels did not decrease. This age-dependent delocalization of BAF from the nucleus to the cytoplasm was also observed in IMR-90 cells and WI-38 cells (supplementary material Fig. S2), suggesting that this phenomenon is general among mortal cells.

As alteration of BAF localization in mortal cells may reflect differences in the time spent in each cell cycle stage during



**Fig. 2.** Age-dependent dislocalization of nuclear BAF in normal cells. (A) Localization of BAF in TIG-1 cells with different ages (left panels). Right panels represent FACS profiles showing cell cycle stages of cells corresponding to the left panels. Scale, 40  $\mu$ m. Arrows represent cells with prominent nuclear signals, the asterisk indicates cells with uniform signaling and arrowheads represent cells with prominent cytoplasmic signals. (B) Proportions of cell populations with different BAF localization: Nuc>Cyto, Nuc=Cyto and Nuc<Cyto represent cells with nucleus-positive, uniform and cytoplasm-positive BAF, respectively. The proportion of cell populations was determined from 19, 11 and 8 independent experiments for cells of PD15, PD47 and PD63, respectively. Data are mean  $\pm$  s.d. of at least 100 cells for each experiment. (C) Western blotting for BAF in young (left) and old (right) TIG-1 cells.

(D) Proportion of cell cycle stages of young proliferating cells with nuclear BAF (nucleus positive and uniform). The proportion of cells with no nuclear BAF (nucleus negative) was less than 1% in young cells, and thus ignored. The results were obtained from 15 independent experiments; at least 100 cells were examined in each experiment. (E) Cell cycle stages of old TIG-1 cells (PD63) with nuclear BAF (corresponding to the nucleus positive and uniform populations) were examined in six independent experiments; at least 100 cells were counted in each experiment. (F) Cell cycle stages of old TIG-1 cells (PD63) with no nuclear BAF (corresponding to the cytoplasm positive population) were examined in five independent experiments; at least 100 cells were counted in each experiment. No S-phase cells were observed in cells with nucleus-negative BAF, suggesting that nuclear BAF is required for S-phase. Data are mean  $\pm$  s.d. for D-F.



aging, we examined cell populations by flow cytometry analysis (Fig. 2A, right panels). The proportion of each cell cycle stage (G1, S and G2-M phase) in young cells of PD15 was 72.9, 17.8 and 9.3%, respectively. Overall, the population of cells in each cell cycle stage was not significantly changed in cells of PD47 and PD63 except that the proportion of S-phase cells was slightly decreased in old cells of PD63 to 13.6% compared with 17.8% in the young cells. To independently determine the population of cells in each cell cycle stage, we used single-cell cytological methods as follows: condensed chromosomes as M phase (stained with a DNA-specific fluorescent dye DAPI), BrdU incorporation as S phase, two separated centrosomes present in a single cell as G2 phase (stained with anti- $\gamma$ -tubulin antibody) and the rest as G1 cells. In young cells, almost all (<99%) of which have nuclear BAF (nucleus positive plus uniform), the proportion of G1, S, G2 and M-phase cells was 42, 32, 24 and 2%, respectively (Fig.

2D). These values were similar to those of old cells with nuclear BAF (Fig. 2E; corresponding to the nucleus-positive and uniform populations in Fig. 2B) although the proportion of cells in S phase was slightly decreased in old cells compared with that of young cells, shown in Fig. 2D. Interestingly, a remarkable feature in the cell cycle stage was observed for the old cells with no nuclear BAF (Fig. 2F; corresponding to the cytoplasm-positive population in Fig. 2B): no S-phase cells were observed in any of the 619 cells examined in five independent experiments. This result strongly suggests that nuclear form of BAF may be required for cell proliferation, especially for S phase, in mortal cells.

#### BAF accumulates in the nucleus during S phase in immortal or cancerous cells

To further understand involvement of nuclear BAF in S phase, we examined the relationship between BAF localization and

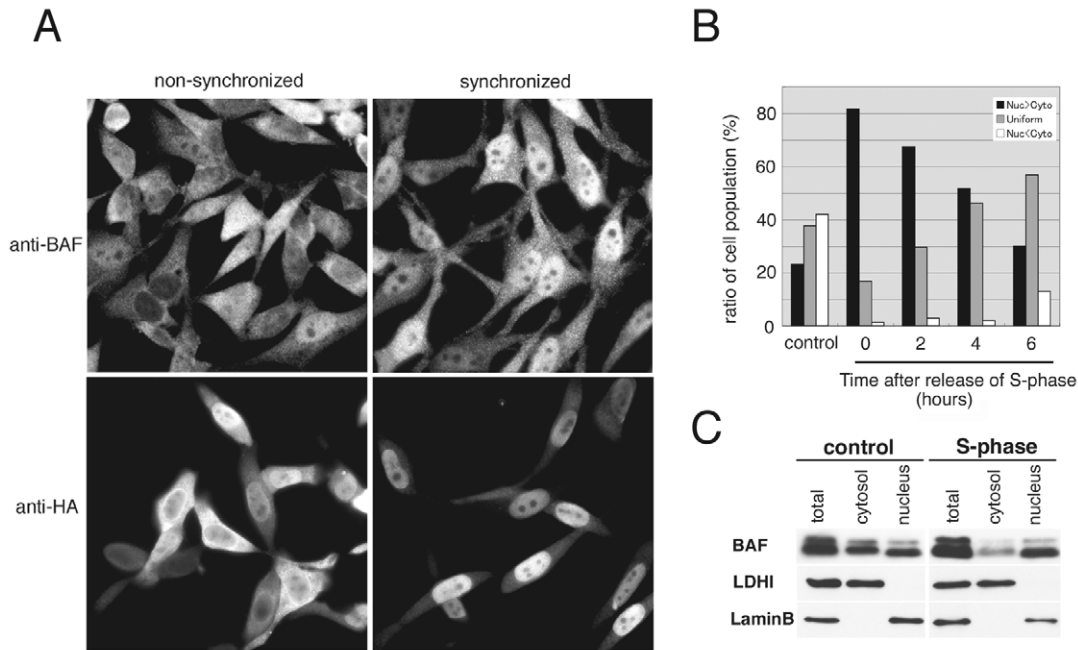


**Fig. 3.** Synchronization at S-phase causes accumulation of BAF in the nucleus. (A) Indirect immunofluorescence staining of endogenous BAF (upper panels) or exogenously expressed HA-BAF (lower panels) in non-synchronized (left panels) and S-phase synchronized (right panels) HeLa cells. Bar, 10  $\mu$ m. (B) Endogenous BAF was stained in non-synchronized (control) and S-phase synchronized HeLa cells 0, 2, 4, and 6 hours after release from the S-phase block. Percentages of the cells with nucleus-positive (black bar), uniform (grey bar) and cytoplasm-positive (white bar) BAF localization patterns are shown. Number of cells examined: 297 for control, 629 for 0 hours, 548 for 2 hours, 714 for 4 hours and 599 for 6 hours. (C) Western blotting analysis using anti-BAF antibody. Whole cell extract (total), the cytoplasmic fraction (cytosol), and the nuclear fraction (nucleus) from non-synchronized (control) and S-phase synchronized (S-phase) HeLa cells were analyzed. Lactate dehydrogenase isoenzyme I (LDHI) and Lamin B were used as markers for cytosol and nucleus, respectively.

the cell cycle stages in various immortal cell lines. HeLa cells or HeLa cells that transiently expressed HA-BAF were synchronized at S phase by sequential treatment with thymidine and hydroxyurea and then imaged by indirect immunofluorescence using antibodies against BAF or HA. In unsynchronized controls, both endogenous BAF and HA-BAF localized heterogeneously, as expected (Fig. 3A, left panels): only 23% of cells were nucleus positive (296 HeLa cells and 69 HA-BAF expressing cells; Fig. 3B). By contrast, the proportion of nucleus-positive cells increased from 23% to 82% in S-phase-arrested cells (Fig. 3A,B). This S-phase dependent nuclear accumulation was also seen in two other immortal cell lines: SiHa and HT-1080 cells (supplementary material Fig. S4), demonstrating that S-phase-dependent nuclear accumulation was not peculiar to HeLa cells. Furthermore, when arrested HeLa cells were released and allowed to resume the cell cycle for 2, 4 and 6 hours, the proportion of nucleus-positive cells progressively decreased to 68%, 52% and 30% (Fig. 3B). These results supported the hypothesis that BAF localization is regulated during the cell cycle in immortal or cancerous cells.

To independently confirm the S-phase-dependent nuclear accumulation of BAF, we used a biochemical strategy: S-phase-arrested HeLa cells were fractionated to separate the nucleus and cytoplasm, then western blotted for BAF (Fig. 3C). BAF was significantly enriched (67%) in the nuclear fraction of S-phase-arrested cells as expected, and evenly distributed between the nucleus and cytoplasm (50% vs 50%) in non-

synchronized cells (Fig. 3C; also see Fig. 1A). To control for potential artifacts of cell synchronization, we determined the localization of BAF as a function of S phase in unsynchronized HeLa cells. To identify S-phase cells we incubated the cells with bromodeoxyuridine (BrdU), and then used double-labeling to detect incorporated BrdU and BAF in each cell. Approximately 80% of BAF nuclear-positive cells (142 cells out of 173 BAF nuclear-positive cells) were also BrdU positive (Fig. 4), demonstrating that nuclear accumulation of BAF correlates with DNA replication. We concluded that in immortal or cancerous cell lines BAF was specifically accumulated in the nucleus during S phase, and thus hypothesized that BAF might have a role in S phase.

#### Loss of BAF delays S-phase progression

To determine whether BAF was required for S phase, we used the RNAi method to downregulate BAF in HeLa cells (BAF-RNAi cells). Three days after RNAi treatment, the proportion of BAF-positive cells dropped to less than 10%, compared with 100% of the control luciferase-RNAi cells, as shown by indirect immunofluorescence staining (Fig. 5A). Quantitative western blotting showed that the BAF RNAi cells expressed only ~10% of BAF present in luciferase-RNAi controls (Fig. 5B). We concluded that our BAF RNAi conditions effectively reduced BAF protein in HeLa cells. In these cells, BAF downregulation did not cause cell death or growth arrest under our experimental conditions, we assume this is because the ~10% residual BAF was sufficient for cell viability. To test the

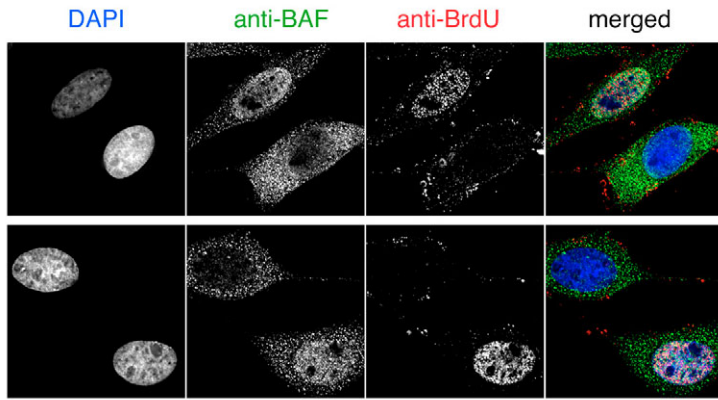
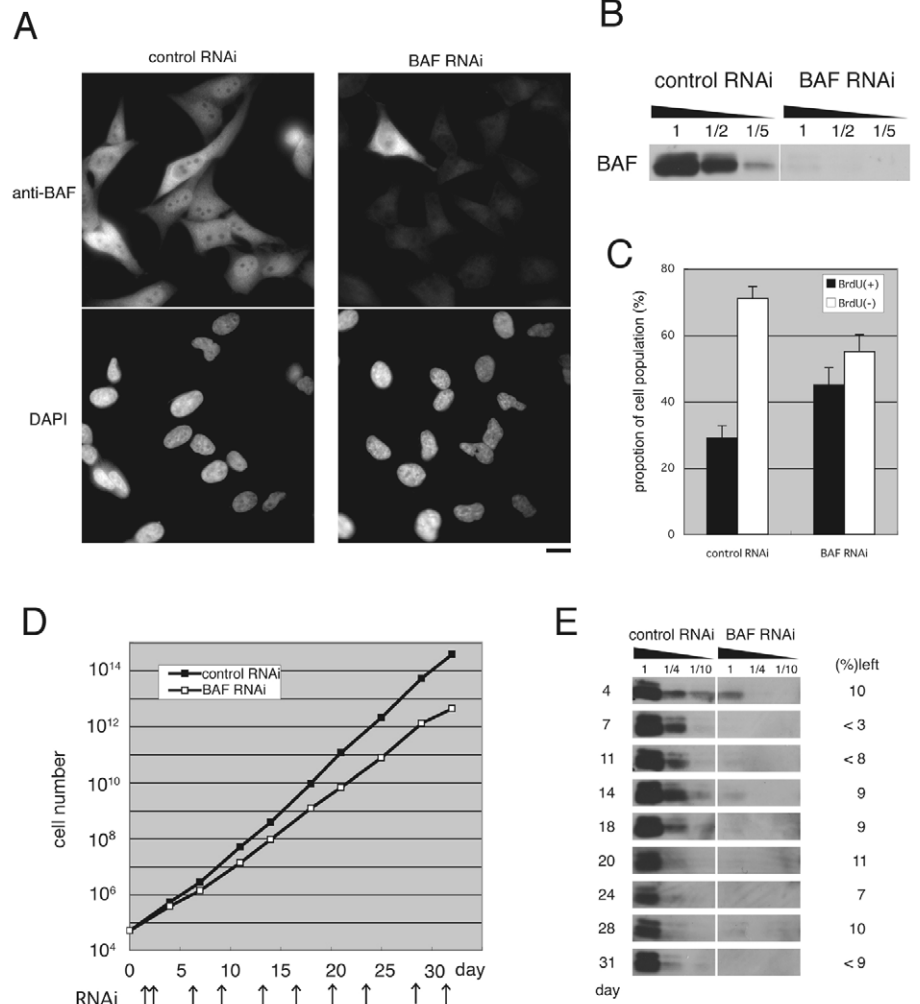


**Fig. 4.** BAF nuclear-positive cells correlate with BrdU-positive cells. Two fields from the same experiment are shown in this figure. Non-synchronized cells were labeled with BrdU, and stained for chromosomes (with DAPI, far left), BAF (second column) and BrdU (third column). The correlation of BAF nuclear-positive cells with BrdU-positive cells was assessed. Of the 467 cells analyzed, 173 cells were BAF nuclear positive; 142 of these cells were BrdU positive. Therefore, 82% of BAF nuclear-positive cells in a non-synchronized population were in S phase (BrdU positive). Merged image (far right) represents chromosomes in blue, anti-BAF in green and anti-BrdU in red. Bar, 10  $\mu$ m.

hypothesized role of BAF in S phase, we used BrdU labeling to quantify the fraction of BAF-RNAi cells that were in S phase, compared with luciferase-RNAi controls. The population of BrdU-positive cells (S-phase cells) was 29% in luciferase-RNAi control cells (Fig. 5C); this number increased

to 45% in BAF-RNAi cells (Fig. 5C). This increase implied a ~4-hour delay in progression through S phase, because the population doubling time was normally ~20 hours (data not shown). Consistent with a prolonged S-phase, the doubling time of BAF RNAi cells was longer (24.8 hours) than control

**Fig. 5.** Loss of BAF by RNAi causes a delay in S-phase progression. (A) Indirect immunofluorescence staining of HeLa cells treated with Luciferase RNAi (control RNAi) or BAF RNAi (BAF RNAi) using Oligofectamine. Cells were stained with anti-BAF antibody-PU38143 for endogenous BAF (upper panels) and DAPI for chromosomes (lower panels). Bar, 20  $\mu$ m. (B) Quantitative western blotting. 25  $\mu$ g (lane 1, extract corresponding to  $5 \times 10^4$  cells), 12.5  $\mu$ g (lane 1/2), and 5  $\mu$ g (lane 1/5) of whole cell extract from cells treated with luciferase RNAi (control RNAi, left three lanes) or BAF RNAi (right three lanes). Endogenous BAF was reduced to approximately 10% of the original amount by RNAi treatment. (C) Cells were treated with luciferase RNAi (control RNAi) or treated with BAF RNAi (BAF RNAi). Cells were then labeled with BrdU. The percentage of cells positive for BrdU (black bars) and negative for BrdU (white bars) is shown. The proportion was represented as a percentage obtained from 19 and 13 independent experiments for control RNAi and BAF RNAi, respectively; more than 260 cells were examined in each experiment. Error bars represent s.d. (D) For long-term RNAi treatment experiments, HeLa cells ( $5 \times 10^4$  in a 35 mm dish at day 0) were transfected with 5–10  $\mu$ g luciferase RNAi (control; closed circles) or BAF RNAi (BAF RNAi; open circles) on day 1 and again on day 2. The cells were subsequently transfected every 3 to 4 days: day 6, 9, 13, 16, 20, 23, 28 and 31. Cell numbers (y-axis) were counted on day 4, 7, 11, 14, 18, 21, 25, 29, 32. Arrows represent the time of RNAi treatment. (E) Western blotting corresponding to Fig. 5D for luciferase RNAi treated cells (left three lanes, control RNAi) and BAF RNAi treated cells (right three lanes, BAF RNAi). 25  $\mu$ g (lane 1, extract corresponding to  $5 \times 10^4$  cells), 6.25  $\mu$ g (lane 1/4), and 2.5  $\mu$ g (lane 1/10) of whole cell extract were applied. Amounts of BAF remaining in BAF RNAi cells are represented on the right as percentages of the control.



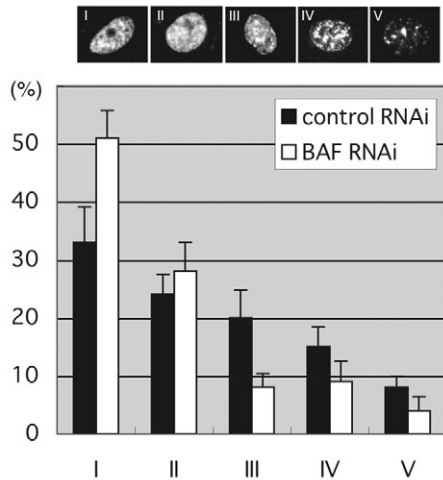


**Fig. 6.** Loss of BAF causes an increase in the number of cells present in the early stages of S phase. HeLa-S3 cells were treated with luciferase RNAi (control RNAi; black bar) or BAF RNAi (BAF RNAi; white bar) using Lipofectamine PLUS and labeled with BrdU. These BrdU-positive cells were classified into five types (I, II, III, IV and V) based on patterns of replication foci as described in O'Keefe et al. (O'Keefe et al., 1992): I for early stage, II for middle, III middle-late, IV for late, and V for late; typical examples are shown in the top panels. The proportion of BrdU-positive cells in each stage was presented as a percentage. Approximately 200 cells were counted for each of 13 independent experiments. The means of the 13 experiments for cells treated with luciferase RNAi (control RNAi) or BAF RNAi (BAF RNAi) are shown. Error bars represent s.d.

luciferase RNAi cells (20.5 hours; Fig. 5D). For this measurement of population doubling time, we used long-term RNAi treatment of up to 32 days (see Materials and Methods and the legend to Fig. 5D). BAF protein levels were less than 10% of the original level throughout this period (Fig. 5E). This 4.3-hour extension in doubling time independently corroborated the 4-hour extension of S phase estimated from the BrdU experiments, strongly supporting the idea that BAF is required for efficient progression through S phase.

Next, to determine which stage of S phase was affected by loss of BAF, we used the classification method based on BrdU staining patterns previously shown to reflect the distribution of DNA replication sites at five different stages of S phase in HeLa cells (O'Keefe et al., 1992). An example of each stage (I, II, III, IV and V) in luciferase-RNAi control nuclei is shown in Fig. 6 (top). The first two stages of S phase (I, II) were over-represented in BAF RNAi cells and the later stages (IV, V) were under-represented compared with luciferase-RNAi controls (~200 cells were counted for each of 13 independent experiments) (Fig. 6). This result suggested BAF was involved in the early stages of S phase.

In *Drosophila*, genetic loss of BAF results in failure to express cyclin A, cyclin B and cyclin E, which are key regulators of the cell cycle (Furukawa et al., 2003). To determine whether a similar mechanism might explain slowed S phase in BAF-RNAi HeLa cells, we measured the expression levels of several cell cycle proteins: cyclin D3 (G1 phase); cyclin E, Cdk2, retinoblastoma (Rb) protein (G1-S transition); cyclin A, PCNA, MCM3, MCM7, CDC6, and CDC7 (S

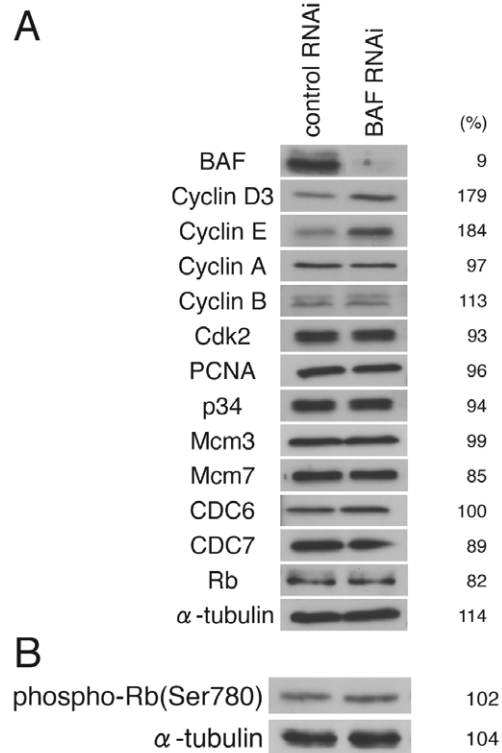


**Fig. 7.** Western blotting analysis for cell-cycle-related proteins. HeLa cells were treated with luciferase RNAi as control (left lane) or BAF RNAi (right lane) using Oligofectamine. 25  $\mu$ g cell extract (corresponding to  $5 \times 10^4$  cells) was analyzed by western blotting using the antibodies indicated on the left. Amounts of corresponding protein in BAF RNAi cells are represented on the right as percentages of the control. Cell extracts were prepared in the homogenizing buffer without (A) or with (B) phosphatase inhibitors.

phase); and cyclin B and p34 (M phase). Western blots of these proteins, with tubulin as a loading control, were carried out in BAF RNAi cells in which BAF was reduced to ~10% of the original amount. Among them, the protein amount of cyclin D3 and cyclin E increased slightly in BAF RNAi cells compared with control luciferase RNAi cells, whereas all other proteins were unchanged (Fig. 7A) and level of Rb phosphorylation was also unchanged (Fig. 7B). These results suggest that loss of BAF does not inhibit an entry to S phase, but may delay progression of S phase.

#### BAF is required for nuclear envelope localization of lamin A

To determine whether reduced expression of BAF affected nuclear assembly or nuclear envelope architecture, we stained BAF RNAi cells by indirect immunofluorescence using antibodies against endogenous emerlin and LAP2 $\beta$  (both nuclear membrane LEM-domain proteins) and lamin A. The signals for all three proteins at the nuclear envelope were significantly weaker than in control luciferase RNAi cells (see Fig. 8B for emerlin and lamin A; data not shown for LAP2 $\beta$ ), whereas nuclear envelope localization of lamin B was unchanged (Fig. 8B). Western blotting showed that the protein levels of emerlin and lamin A/C were unchanged (Fig. 8A).



Thus, these proteins were either mislocalized or epitope masked in cells with reduced BAF. We favor the mislocalization theory, because BAF was previously shown to be important to assemble both emerin and lamin A into the reforming nuclear envelope (Haraguchi et al., 2001). Further supporting this point, BAF is also suggested to stabilize emerin binding to lamin A (Bengtsson and Wilson, 2006). It is also worth mentioning that exogenous LAP2 $\beta$  was shown to increase DNA replication efficiency in nuclei assembled in *Xenopus* egg extracts (Gant et al., 1999). Collectively, our

findings suggest that loss of BAF might affect S-phase progression either directly, or indirectly via mislocalization of A-type lamins, LAP2 $\beta$  or as yet unknown S-phase factors.

### Discussion

It has been reported that BAF shows heterogenous, and sometimes inconsistent, localization patterns in cells. We found that BAF localization varied depending on the mortal or immortal status of the cell. BAF remained in the nucleus throughout interphase of the cell cycle in young proliferating cells of mortal cell lines (Fig. 1C, Fig. 2A). Such nucleus-only localization has also been reported in rat FRSK cells, a cultured cell line of fetal rat epidermal keratinocytes (Furukawa, 1999). By contrast, high levels of cytoplasmic BAF were observed in immortal cell types HeLa-S3 and A431 (Fig. 1C). This cytoplasmic localization is consistent with the fact that BAF was first purified from cytoplasmic fractions (Lee and Craigie, 1998). Our experimental findings provide insight into this phenomenon. Unlike young proliferating cells, BAF is mostly localized in the cytoplasm in older senescing TIG-1 cells. These older cells reside primarily in the G1 or G2 phases of the cell cycle. We therefore suggest that BAF exit from the nucleus during G1 and/or G2 phase may be required for normal

progression into senescence. In our current model, cancer is proposed to arise in cells that can both express oncogenes and avoid oncogene-induced senescence (reviewed by Hemann and Narita, 2007). We found that BAF localizes significantly in the cytoplasm in both senescent mortal cells and cancerous immortal cells, leading us to speculate that nuclear BAF might suppress both senescence and cancer progression. Obviously, further studies are needed to elucidate the difference and significance of BAF localization in mortal vs immortal cells, especially regarding control of cellular proliferation.

What is the molecular basis for the heterogenous localization patterns in cells? BAF interacts with many binding partners (see Introduction), and these interactions may influence its localization. This

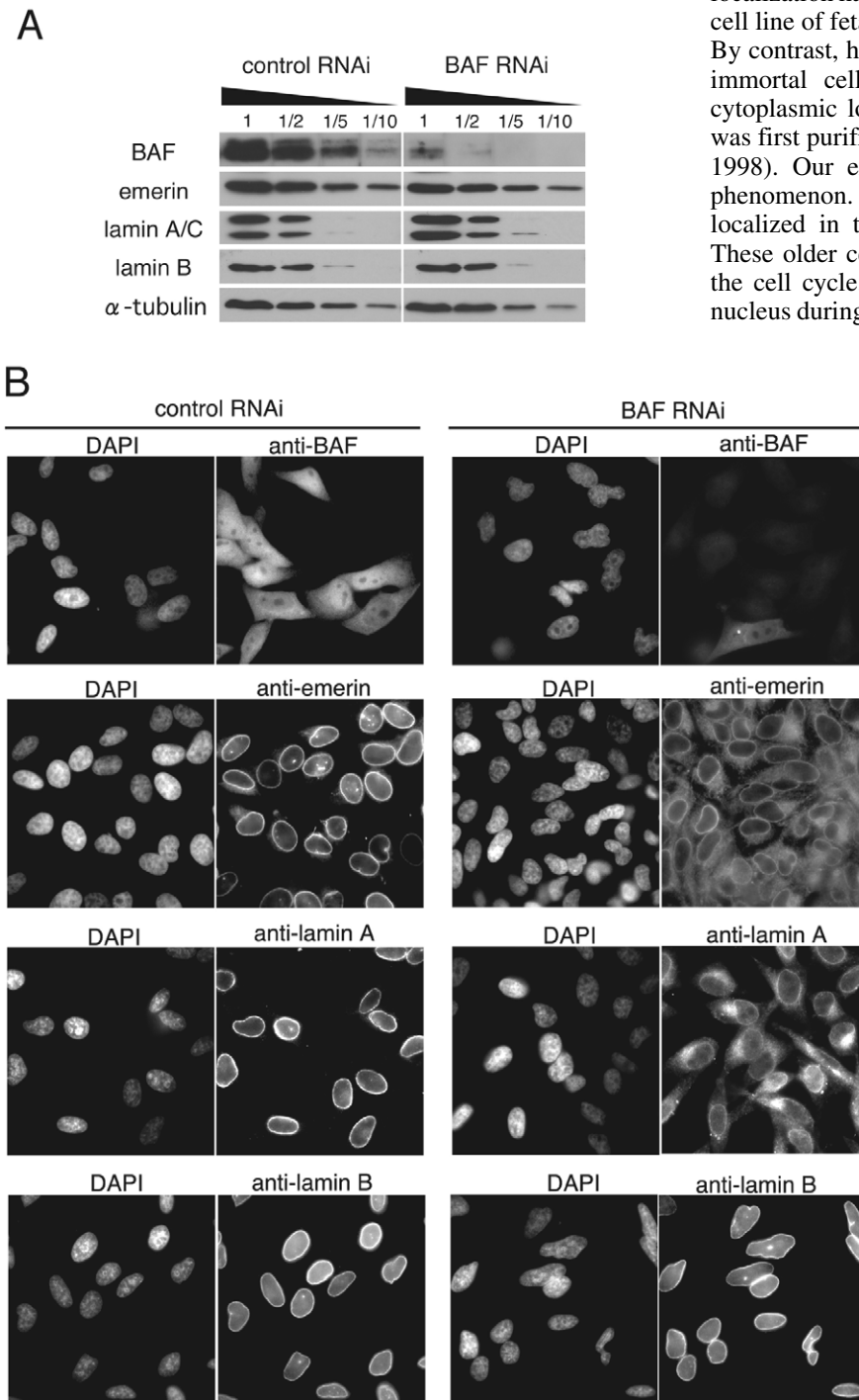


**Fig. 8.** Loss of BAF causes disassembly of emerin and lamin A from the nuclear envelope. (A) Quantitative western blotting using the antibodies indicated on the left. 25  $\mu$ g (lane 1, extract corresponding to  $5 \times 10^4$  cells), 12.5  $\mu$ g (lane 1/2), 5  $\mu$ g (lane 1/5), 2.5  $\mu$ g (lane 1/10) of whole cell extract from cells treated with luciferase RNAi (control RNAi, left) or BAF RNAi (right) using Oligofectamine. Upper and lower bands in lamin A/C are lamin A and lamin C, respectively. (B) Indirect immunofluorescence staining using anti-BAF, anti-emerin, anti-lamin A, and anti-lamin B antibodies of cells treated with luciferase RNAi (control RNAi; left panels) or BAF RNAi (BAF RNAi; right panels). Chromosomes were stained with DAPI. Bar, 20  $\mu$ m.



hypothesis is supported by our findings that loss of lamin A by RNAi caused loss of nuclear localization of both endogenous BAF and GFP-BAF in HeLa cells (data not shown), and a previous finding that double knockdown of EMR-1 (emerin) and LEM-2 (LEM-domain protein) in *C. elegans* embryos caused reduction of BAF localization to the nuclear envelope (Liu et al., 2003). In addition to binding partners, post-translational modification of BAF itself may also influence its localization. BAF is phosphorylated at Ser4 both in vitro and in vivo (Bengtsson and Wilson, 2006; Gorjánác et al., 2006). A host-cell-encoded protein, vaccinia-related kinase (VRK) 1, can phosphorylate BAF in vitro at three N-terminal residues (Thr2, Thr3 and Ser4; TTS), and co-expression of VRK1 with GFP-BAF in HeLa cells changed the localization of GFP-BAF from the nucleus to the cytoplasm (Nichols et al., 2006). In addition, it has been reported that depletion of VRK-1 (VRK1 homolog in *C. elegans*) by RNAi in *C. elegans* embryos caused accumulation of BAF-1 (BAF homolog in *C. elegans*) on chromatin throughout all cell cycle stages including mitosis (Gorjánác et al., 2006). These findings suggest that VRK1 kinase may be one of the factors responsible for modulating BAF localization (i.e. in the nucleus or cytoplasm) and also suggests that the expression level or activity of VRK1 in individual cell lines may be one determinant of BAF localization. This hypothesis can be tested by examining the amount of VRK1 in various cell lines, and examining the effect of depletion of VRK1 by RNAi.

We also demonstrated that BAF localization was regulated during the cell cycle in immortal/cancerous cells. In immortal cells, BAF accumulated in the nucleus during S phase of the cell cycle. Such cell-cycle-dependent re-localization of BAF was not obvious in mortal cell lines, especially in young proliferating cells. In these cells, BAF remained in the nucleus throughout interphase of the cell cycle. However, BAF is frequently lost from the nucleus in old cells, and, importantly, cells without nuclear BAF were never found to be actively progressing through S phase (Fig. 2F). These findings suggest a necessary role for nuclear BAF in cell proliferation in mortal cells as well as in immortal cells. The mechanism(s) by which S-phase might depend on BAF remains unknown, but possibilities include (1) genes that might be regulated directly or indirectly by BAF; (2) BAF interactions with histones that influence chromatin structure (Montes de Oca et al., 2005); or (3) indirect mechanisms involving roles of BAF in stabilizing nuclear lamina architecture. Because western blotting analysis revealed that cells with ~10% residual levels of BAF had apparently normal expression of S-phase proteins including PCNA, MCM family proteins, CDC6 and CDC7, one might predict that BAF may be indirectly involved in S-phase events. For example, BAF may affect nuclear architecture that is required for DNA replication. One such factor may be the nuclear lamina; B-type lamins are essential for DNA replication in *Xenopus* egg extract systems (Meier et al., 1991). Reduced levels of BAF disrupted nuclear lamin A and, although A-type lamins are not required for DNA replication, BAF-mediated disruption of A-type lamins might indirectly disrupt functions associated with B-type lamins. LAP2 $\beta$  is another possible factor, because although it increases DNA replication efficiency in nuclei assembled in *Xenopus* egg extracts (Gant et al., 1999), it was mislocalized from the nucleus in BAF-downregulated cells.

In *Drosophila*, genetic knockout of BAF causes S-phase defects in proliferating cells of the central nervous system, resulting in lethality at the larval-pupal transition during development (Furukawa et al., 2003). These S-phase defects resemble our observation in human mortal cells. In *Drosophila*, however, it has been found that cyclin A, cyclin B and cyclin E were all downregulated by loss of BAF (Furukawa et al., 2003) whereas our results in HeLa cells showed that cyclin A and cyclin B were unchanged and cyclin D3 and cyclin E were slightly upregulated in BAF-depleted cells (Fig. 7). It has been shown that overexpression of LAP2 $\alpha$ , a major intranuclear LEM-domain protein, upregulates the expression of cyclin D1 and cyclin E in mouse NIH3T3 cells, and leads to differentiation by inhibiting Rb phosphorylation (Dorner et al., 2006). Because LAP2 $\alpha$  binds BAF (Dechat et al., 2004) (T.H., unpublished observation) and because both are relatively abundant, loss of BAF may have downstream effects on LAP2 $\alpha$  by increasing the effective concentration of 'free' (non-BAF-bound) LAP2 $\alpha$ . The human-cell-specific phenotype may be attributed to species-specific proteins such as LAP2 $\alpha$ , a mammalian-specific BAF-binding protein, which does not exist in *Drosophila*.

In conclusion, our findings suggest that BAF may be a modulator of cell proliferation by influencing S-phase progression. Many nuclear envelope proteins including BAF, lamin A, and emerin do not exist in unicellular eukaryotes such as yeasts, but appear evolutionarily in multicellular metazoans including *C. elegans*. In multicellular organisms, DNA synthesis and/or cell proliferation can be selectively regulated in individual cells or cell types to produce specific tissues and organs, and BAF may modulate these events through interaction with nuclear envelope proteins.

## Materials and Methods

### Cells

TIG-1 cells (primary normal diploid cells isolated from 5-month-old fetal lung) were a gift from H. Kondo (Tokyo Metropolitan Institute of Gerontology, Tokyo, Japan). HeLa cells (established from cervical carcinoma, epithelial-like), and A431 cells (established from epidermoid carcinoma, epithelial-like) were obtained from the Riken Cell Bank (Tsukuba Science City, Tsukuba, Japan). IMR-90 cells (primary normal diploid cell line from lung, fibroblast-like), WI-38 (primary normal diploid cell from lung, fibroblast-like), KMRC-1 cells (clear cell renal carcinoma cell line isolated from kidney, epithelial-like), KMRC-2 cells (clear cell renal carcinoma cell line isolated from kidney cancer, fibroblast-like), Hep G2 cells (hepatoma cell line isolated from liver cancer) and RERF-LC-KJ cells (adenocarcinoma from lung cancer, epithelial-like) were from Health Science Research Resources Bank (JCRB). HeLa-S3 cells (a variant of HeLa cells), SiHa cells (established from uterus cancer, epithelial-like), and HT-1080 cells (established from fibrosarcoma) were provided by N. Imamoto (RIKEN, Japan), M. Noda (Kyoto University, Japan) and H. Masumoto (Nagoya University, Japan), respectively. Clones of HeLa cells stably expressing GFP-BAF were selected as described previously (Shimi et al., 2004).

TIG-1 cells were maintained strictly according to the method developed by the original developer (Ohashi et al., 1980). Cells were plated in a 6-cm culture dish (25% confluent) and incubated in minimum essential medium (MEM) supplemented with 10% calf serum at 37°C in a CO<sub>2</sub> incubator (under 5% CO<sub>2</sub> gas) for 1 week with a single medium change at 3-4 days. After 1 week, proliferating cells had become confluent and were passaged again. Using this protocol, one passage equates to two population doublings (PD). WI-38 and IMR-90 cells were also maintained under the same culture conditions as TIG-1 cells. Young proliferative cells of relatively low PD grow to confluence in a couple of days; proliferation is stopped by contact inhibition. By later passages (PD>62) older TIG-1 cells had stopped proliferating and did not reach confluence. HeLa cells and HeLa S-3 cells were maintained in DME medium supplemented with 10% calf serum; RERF-LC-KJ cells in RPMI1640 medium supplemented with 10% fetal bovine serum; and KMRC-1 cells, KMRC-2 cells, HT-1080 cells, A431 cells, Hep-G2 cells and SiHa cells in DME medium supplemented with 10% fetal bovine serum. These cell lines were passaged every 3 or 4 days.

## Reagents

Double-stranded siRNA for BAF and lamin A were purchased from Qiagen (Hiden, Germany). 5'-bromo-2' deoxyuridine, and anti-lamin B antibody (Ab-1) were from Calbiochem (La Jolla, CA). Anti-human lactate dehydrogenase isoenzyme I (LDHI) was from The Binding Site (Birmingham, UK). Mouse monoclonal anti-bromodeoxyuridine antibody (Ab-2) was from Oncogene Research Products (Boston, MA). Mouse monoclonal anti-cyclin D3 antibody (DCS-22), rabbit polyclonal anti-cyclin A antibody (Ab-7), rabbit polyclonal anti-cyclin E antibody (Ab-1) and mouse monoclonal anti-Cdk2 antibody (2B6) were from Lab vision corporation (Fremont, CA). Mouse monoclonal anti-Rb antibody (3H9), anti-PCNA antibody (5A10), anti-CDC6 antibody (DCS-180), anti-CDC7 antibody (DCS-342), anti-MCM3 antibody (3A2) and anti-MCM7 antibody (4B4) were from MBL (Nagoya, Japan). Affinity-purified rabbit polyclonal anti-cyclin B1 antibody (H-433) was from Santa Cruz Biotechnology (Santa Cruz, CA). Mouse monoclonal anti- $\alpha$ -tubulin antibody (B-5-1-2) was from Sigma (Saint Louis, MO). Mouse monoclonal anti-lamin A/C antibody (clone XB10) and mouse monoclonal anti-HA antibody (clone 16B12) were from Covance (Berkeley, CA). Mouse monoclonal anti-p34 antibody was a gift from Dr Yamashita (Yamashita et al., 1991).

Two affinity-purified anti-BAF antibodies were used for this study. One was from rabbit polyclonal serum anti-BAF-PU38143 generated against recombinant BAF. The other was from rabbit polyclonal serum anti-BAF-3273-6 (a gift from K. L. Wilson, Johns Hopkins University) produced against a synthetic peptide as described previously (Haraguchi et al., 2001). Specific antibodies were affinity-purified from these sera as follows. Rabbit serum (20–50  $\mu$ l) was incubated in PBS for 3 hours at room temperature with filter paper onto which approximately 10  $\mu$ g of purified recombinant BAF protein was pre-absorbed. After removal of unbound fractions, the filter paper was washed three times with PBS and treated with 500  $\mu$ l of 100 mM glycine (pH 2.5) to elute BAF-specific antibodies. Eluted antibodies were neutralized with 1 M Tris-HCl, and then concentrated to their original volume by centrifugation in a Centricon-30 (Amicon), replacing the solution with PBS. Both affinity-purified antibodies specifically recognized BAF by western blot analysis.

## Plasmid construction

To construct HA-BAF plasmids, the coding region of BAF was PCR amplified and digested with *Bam*HI and inserted into a p3HA-C1 vector (pCM530) containing a *Bg*III site. The DNA sequences of all fusion plasmids were confirmed using an ABI 310 or ABI 3100 Genetic Analyser (Applied Biosystems, Norwalk, CT).

## Transfection of DNA plasmid

Cells cultured in a 35 mm glass-bottom culture dish were transfected with 0.2  $\mu$ g of plasmid DNA using Lipofectamine PLUS (Invitrogen, Carlsbad, CA). After transfection, cells were cultured for 2 days and then fixed with a mixture of 0.2% glutaraldehyde and 3.7% formaldehyde for 15 minutes at room temperature. Indirect immunofluorescence staining was performed as described below except that anti-HA antibody (Covance, Richmond, CA) was used as the primary antibody.

## Indirect immunofluorescence staining

Cells were cultured in a glass bottom culture dish and then fixed with a mixture of 0.2% glutaraldehyde and 3.7% formaldehyde for 15 minutes at room temperature as described previously (Haraguchi et al., 2000; Haraguchi et al., 2001). After washing with PBS three times, the cells were treated with 0.1% Triton X-100 in PBS for 5 minutes at room temperature and washed with PBS three times. The cells were then treated with 0.1% sodium borohydride in PBS for 15 minutes at room temperature to block unreacted glutaraldehyde, washed with PBS three times, and treated with 1% BSA in PBS for 1 hour. After removal of the BSA solution, the cells were incubated for 20 hours at 4°C in affinity-purified anti-BAF antibody (see Cells and Reagents and Fig. 1) at a dilution of 1:500 (diluted with 1% BSA-PBS). The cells were then washed four times with PBS and treated with Alexa Fluor 488-conjugated secondary antibody (Molecular Probes) at a dilution of 1:1000 for 3–4 hours at room temperature. The cells were then washed three times with PBS and mounted in 90% glycerol. TCA fixation was also used as described previously (Haraguchi et al., 2004) except that anti-BAF antibody was used as the primary antibody.

## Labeling of S-phase cells with bromodeoxyuridine

Cells were cultured in the presence of 200  $\mu$ M bromodeoxyuridine (BrdU) for 30 minutes, washed with DME medium supplemented with 10% calf serum, fixed with a mixture of 0.2% glutaraldehyde, 3.7% formaldehyde for 20 minutes, treated with either methanol or 0.1% Triton X-100 in PBS for 5 minutes, and then treated twice with 0.1% sodium borohydride for 15 minutes. The cells were then incubated with 1% BSA in PBS for 1 hour followed by incubation with anti-BAF antibody (1:200 dilution), anti-BrdU antibody (1:100), 10  $\mu$ g/ml DNase I, and 0.3 mM MgCl<sub>2</sub> for 20 hours at 4°C. After washing with PBS three times, the cells were treated with Alexa Fluor 488-conjugated anti-rabbit antibody (1:2000 dilution) for BAF or Cy3-conjugated anti-mouse antibody (1:2000 dilution) for BrdU for 3 hours at room temperature. After washing with PBS three times, the cells were mounted in 90% glycerol as described (Haraguchi et al., 2001) and observed by a DeltaVision microscope system. The BrdU-positive cells were classified into five stages (I, II,

III, IV and V) corresponding to the temporal order of chromatin replication, based on patterns of BrdU incorporation (O'Keefe et al., 1992). Briefly, stage I is characterized by relatively uniform distribution in the nucleoplasm except for the nucleolus, stage II by weaker staining on euchromatic regions and stronger staining on heterochromatic regions, stage III by stronger staining of perinucleolar chromatin and perinuclear heterochromatin, stage IV by interconnecting patches, and stage V by a few large foci.

## Fluorescence microscopy

Fluorescence microscope images were obtained with a DeltaVision microscope system (Applied Precision, Seattle, WA) (Haraguchi et al., 2001). Optical section data (15–30 focal planes at 0.5  $\mu$ m intervals) were collected on a Peltier-cooled charge-coupled device (CH350, Photometrics, Tucson, AZ) using an oil-immersion objective lens (PlanApo 60, NA=1.4) on an Olympus microscope IX70, and computationally processed by a deconvolution method using standard software on the Delta Vision microscope system (Agard et al., 1989).

## Flow cytometry analysis

HeLa cells were harvested and fixed with 70% ethanol at –20°C for overnight; after fixation, cells were washed with PBS containing 0.2% BSA. To measure DNA contents, fixed cells were treated with 0.05 mg/ml RNase A (Wako) in PBS containing 0.2% BSA for 30 minutes at room temperature, and then stained with 0.05 mg/ml propidium iodide (Sigma) for 10 minutes at room temperature. DNA content was measured on a flow cytometer EPICS XL (Beckman Coulter); cell cycle stages were analyzed using the software EXPO32 and MultiCycle (Beckman Coulter).

## Synchronization of cells in S phase

HeLa cells were grown in DMEM culture medium plus 10% calf serum. Thymidine was added to a final concentration of 2.5 mM, and the cells were incubated 24 hours. After washing with PBS twice, the cells were cultured for 10 hours in fresh medium (DMEM + 10% calf serum). Then hydroxyurea was added to a final concentration of 1 mM, and the cells were cultured for 14 hours. To release the S-phase block, the cells were washed twice with PBS, then given fresh medium and incubated until they were processed for immunofluorescence or western blot analyses.

## Western blotting

HeLa cells ( $1 \times 10^7$ ) were washed twice with DMEM, collected by scraping with a rubber policeman, suspended in homogenizing buffer (20 mM Tris-HCl, pH 7.5, 2 mM MgCl<sub>2</sub>, 150 mM NaCl) supplemented with protease inhibitor cocktail (Roche) to a final concentration of  $2 \times 10^7$  cells/ml, and then homogenized on ice using a Potter homogenizer. Phosphatase inhibitor cocktail (Sigma) was added to the homogenizing buffer only in experiments of Rb phosphorylation. Half of each sample was centrifuged at 1000 g for 3 minutes to separate the nuclear (pellet) and cytoplasmic (supernatant) fractions, and the other half was kept as the 'total lysate' fraction. Sample fractions were boiled for 5 minutes in SDS sample buffer and then fresh dithiothreitol (DTT) was added to a final concentration of 2 mM. This addition of DTT before electrophoresis was crucial for resolving BAF bands. Samples corresponding to  $1 \times 10^5$  cells were loaded per lane of an SDS 15% polyacrylamide gel. After electrophoresis, proteins were transferred to a PVDF membrane at 2 mA/cm<sup>2</sup> for 1.5 hours in transfer buffer (50 mM Tris-HCl pH 7.5, 380 mM glycine and 20% methanol) in the absence of SDS. After blocking with 5% skimmed milk in PBS, the membrane was incubated at 4°C overnight with a rabbit polyclonal anti-BAF serum (unless otherwise specified) at a dilution of 1:1000 in PBS containing 0.1% skimmed milk and 0.1% Tween-20. After washing with PBS, blots were incubated at 4°C for 3 hours with horseradish peroxidase (HRP)-conjugated anti-rabbit IgG (Cappel) at a dilution of 1:1000, and stained by enhanced chemiluminescence (Amersham Biosciences). To examine the efficiency of fractionation, anti-lamin B antibody and anti-LDHI antibody were also western blotted as markers for the nucleus and cytoplasm, respectively.

## Knockdown by RNA interference (RNAi)

5–10  $\mu$ g of double-stranded RNA oligonucleotides for BAF (AAGAAGCTGGA-GGAAAGGGGT) was transfected into HeLa cells cultured in a 35 mm culture dish using Oligofectamine (Invitrogen), or Lipofectamine Plus (Invitrogen) transfection reagents according to the manufacturer's instructions: These transfection reagents and methods worked equally well, and the reagent used was specified in the figure legend. Cells were incubated for 3 days in DMEM culture medium containing 10% fetal bovine serum, and then used for further analyses. For long-term RNAi treatment experiments, cells ( $5 \times 10^4$  in a 35 mm dish at day 0) were transfected with 5–10  $\mu$ g double-stranded RNA on day 1 and again on day 2, and the transfection procedure was subsequently repeated every 3–4 days thereafter (see the legend to Fig. 5D,E).

We are grateful to Hiroshi Kondo (Tokyo Metropolitan Institute of Gerontology, Tokyo, Japan) for TIG-1 cells and Masakane Yamashita (Hokkaido University, Japan) for anti-p34 antibody. Especially we

thank Katherine L. Wilson (Johns Hopkins University, USA) for providing anti-BAF antibody and valuable discussion throughout this research. We also thank David B. Alexander for comments on the paper, Satoshi Tashiro (Hiroshima University) for sharing his method of BrdU labelling, and Katsuzumi Okumura (Mie University) for communicating DNA replication results prior to publication. This work was supported by grants from the Japan Science and Technology Agency (CREST; to T.H. and Y.H.) and Grant-in-Aid for Scientific Research A (to T.H.) from Ministry of Education, Science and Sports of Japan.

## References

- Agard, D. A., Hiraoka, Y., Shaw, P. and Sedat, J. W. (1989). Fluorescence microscopy in three dimensions. *Methods Cell Biol.* **30**, 353-377.
- Bengtsson, L. and Wilson, K. L. (2006). Barrier-to-autointegration factor phosphorylation on Ser-4 regulates emerin binding to lamin A in vitro and emerin localization in vivo. *Mol. Biol. Cell* **17**, 1154-1163.
- Brachner, A., Reipert, S., Foisner, R. and Gotzmann, J. (2005). LEM2 is a novel MAN1-related inner nuclear membrane protein associated with A-type lamins. *J. Cell Sci.* **118**, 5797-5810.
- Bradley, C. M., Ronning, D. R., Ghirlando, R., Cragie, R. and Dyda, F. (2005). Structural basis for DNA bridging by barrier-to-autointegration factor. *Nat. Struct. Mol. Biol.* **12**, 935-936.
- Cai, M., Huang, Y., Zheng, R., Wei, S. Q., Ghirlando, R., Lee, M. S., Cragie, R., Gronenborn, A. M. and Clore, G. M. (1998). Solution structure of the cellular factor BAF responsible for protecting retroviral DNA from autointegration. *Nat. Struct. Biol.* **5**, 903-909.
- Dechat, T., Vlcek, S. and Foisner, R. (2000). Review: lamina-associated polypeptide 2 isoforms and related proteins in cell cycle-dependent nuclear structure dynamics. *J. Struct. Biol.* **129**, 335-345.
- Dechat, T., Gajewski, A., Korbei, B., Gerlich, D., Daigle, N., Haraguchi, T., Furukawa, K., Ellenberg, J. and Foisner, R. (2004). LAP2alpha and BAF transiently localize to telomeres and specific regions on chromatin during nuclear assembly. *J. Cell Sci.* **117**, 6117-6128.
- Dorner, D., Vlcek, S., Foeger, N., Gajewski, A., Makolm, C., Gotzmann, J., Hutchison, C. J. and Foisner, R. (2006). Lamina-associated polypeptide 2alpha regulates cell cycle progression and differentiation via the retinoblastoma-E2F pathway. *J. Cell Biol.* **173**, 83-93.
- Foisner, R. (2001). Inner nuclear membrane proteins and the nuclear lamina. *J. Cell Sci.* **114**, 3791-3792.
- Furukawa, K. (1999). LAP2 binding protein 1 (L2BP1/BAF) is a candidate mediator of LAP2-chromatin interaction. *J. Cell Sci.* **112**, 2485-2492.
- Furukawa, K., Sugiyama, S., Osouda, S., Goto, H., Inagaki, M., Horigome, T., Omata, S., McConnell, M., Fisher, P. A. and Nishida, Y. (2003). Barrier-to-autointegration factor plays crucial roles in cell cycle progression and nuclear organization in *Drosophila*. *J. Cell Sci.* **116**, 3811-3823.
- Gant, T. M., Harris, C. A. and Wilson, K. L. (1999). Roles of LAP2 proteins in nuclear assembly and DNA replication: truncated LAP2beta proteins alter lamina assembly, envelope formation, nuclear size, and DNA replication efficiency in *Xenopus laevis* extracts. *J. Cell Biol.* **144**, 1083-1096.
- Gorjánác, M., Klerkx, E. P., Galy, V., Santarella, R., López-Iglesias, C., Askjaer, P. and Mattaj, I. W. (2007). *Caenorhabditis elegans* BAF-1 and its kinase VRK-1 participate directly in post-mitotic nuclear envelope assembly. *EMBO J.* **26**, 132-143.
- Haraguchi, T., Koujin, T., Hayakawa, T., Kaneda, T., Tsutsumi, C., Imamoto, N., Akazawa, C., Sukegawa, J., Yoneda, Y. and Hiraoka, Y. (2000). Live fluorescence imaging reveals early recruitment of emerin, LBR, RanBP2, and Nup153 to reforming functional nuclear envelopes. *J. Cell Sci.* **113**, 779-794.
- Haraguchi, T., Koujin, T., Segura, M., Lee, K. L., Matsuoka, Y., Yoneda, Y., Wilson, K. L. and Hiraoka, Y. (2001). BAF is required for emerin assembly into the reforming nuclear envelope. *J. Cell Sci.* **114**, 4575-4585.
- Haraguchi, T., Holaska, J. M., Yamane, M., Koujin, T., Hashiguchi, N., Mori, C., Wilson, K. L. and Hiraoka, Y. (2004). Emerin binding to Btf, a death-promoting transcriptional repressor, is disrupted by a missense mutation that causes Emery-Dreifuss muscular dystrophy. *Eur. J. Biochem.* **271**, 1035-1045.
- Hemann, M. T. and Narita, M. (2007). Oncogenes and senescence: breaking down in the fast lane. *Genes Dev.* **21**, 1-5.
- Holaska, J. M., Lee, K. K., Kowalski, A. K. and Wilson, K. L. (2003). Transcriptional repressor germ cell-less (GCL) and barrier to autointegration factor (BAF) compete for binding to emerin in vitro. *J. Biol. Chem.* **278**, 6969-6975.
- Jacque, J.-M. and Stevenson, M. (2006). The inner-nuclear-envelope protein emerin regulates HIV-1 infectivity. *Nature* **441**, 641-645.
- Lee, K. K. and Wilson, K. L. (2004). All in the family: evidence for four new LEM-domain proteins Lem2 (NET-25), Lem3, Lem4 and Lem5 in the human genome. *Symp. Soc. Exp. Biol.* **56**, 329-339.
- Lee, M. S. and Cragie, R. (1994). Protection of retroviral DNA from autointegration: involvement of a cellular factor. *Proc. Natl. Acad. Sci. USA* **91**, 9823-9827.
- Lee, M. S. and Cragie, R. (1998). A previously unidentified host protein protects retroviral DNA from autointegration. *Proc. Natl. Acad. Sci. USA* **95**, 1528-1533.
- Lin, F., Blake, D. L., Callebaut, I., Skerjanc, I. S., Holmer, L., McBurney, M. W., Paulin-Levasseur, M. and Worman, H. J. (2000). MAN1, an inner nuclear membrane protein that shares the LEM domain with lamina-associated polypeptide 2 and emerin. *J. Biol. Chem.* **275**, 4840-4847.
- Liu, J., Lee, K. K., Segura-Totten, M., Neufeld, E., Wilson, K. L. and Gruenbaum, Y. (2003). MAN1 and emerin have overlapping function(s) essential for chromosome segregation and cell division in *Caenorhabditis elegans*. *Proc. Natl. Acad. Sci. USA* **100**, 4598-4603.
- Margalit, A., Segura-Totten, M., Gruenbaum, Y. and Wilson, K. L. (2005). Barrier-to-autointegration factor is required to segregate and enclose chromosomes within the nuclear envelope and assemble the nuclear lamina. *Proc. Natl. Acad. Sci. USA* **102**, 3290-3295.
- Meier, J., Campbell, K. H., Ford, C. C., Stick, R. and Hutchison, C. J. (1991). The role of lamin LIII in nuclear assembly and DNA replication, in cell-free extracts of *Xenopus* eggs. *J. Cell Sci.* **98**, 271-279.
- Montes de Oca, R., Lee, K. and Wilson, K. L. (2005). Binding of barrier-to-autointegration factor (BAF) to histone H3 and selected linker histones including H1.1. *J. Biol. Chem.* **280**, 42252-42262.
- Nichols, R. J., Wiebe, M. S. and Traktman, P. (2006). The vaccinia-related kinases phosphorylate the N' terminus of BAF, regulating its interaction with DNA and its retention in the nucleus. *Mol. Biol. Cell* **17**, 2451-2464.
- Ohashi, M., Aizawa, S., Ooka, H., Ohsawa, T., Kaji, K., Kondo, H., Kobayashi, T., Noumura, T., Matsuo, M., Mitsui, Y. et al. (1980). A new human diploid cell strain, TIG-1, for the research on cellular aging. *Exp. Gerontol.* **15**, 121-133.
- O'Keefe, R. T., Henderson, S. C. and Spector, D. L. (1992). Dynamic organization of DNA replication in mammalian cell nuclei: spatially and temporally defined replication of chromosome-specific alpha-satellite DNA sequences. *J. Cell Biol.* **116**, 1095-1110.
- Segura-Totten, M. and Wilson, K. L. (2004). BAF: roles in chromatin, nuclear structure and retrovirus integration. *Trends Cell Biol.* **14**, 261-266.
- Segura-Totten, M., Kowalski, A. K., Cragie, R. and Wilson, K. L. (2002). Barrier-to-autointegration factor: major roles in chromatin decondensation and nuclear assembly. *J. Cell Biol.* **158**, 475-485.
- Schirmer, E. C., Florens, L., Guan, T., Yates, J. R., 3rd and Gerace, L. (2003). Nuclear membrane proteins with potential disease links found by subtractive proteomics. *Science* **301**, 1380-1382.
- Tift, K. E., Segura-Totten, M., Lee, K. K. and Wilson, K. L. (2006). Barrier-to-autointegration factor-like (BAF-L): a proposed regulator of BAF. *Exp. Cell Res.* **312**, 478-487.
- Shimi, T., Koujin, T., Segura-Totten, M., Wilson, K. L., Haraguchi, T. and Hiraoka, Y. (2004). Dynamic interaction between BAF and emerin revealed by FRAP, FLIP, and FRET analyses in living HeLa cells. *J. Struct. Biol.* **147**, 31-41.
- Shumaker, D. K., Lee, K. K., Tanheco, Y. C., Cragie, R. and Wilson, K. L. (2001). LAP2 binds to BAF-DNA complexes: requirement for the LEM-domain and modulation by variable regions. *EMBO J.* **20**, 1754-1764.
- Suzuki, Y., Yang, H. and Cragie, R. (2004). LAP2alpha and BAF collaborate to organize the Moloney murine leukemia virus preintegration complex. *EMBO J.* **23**, 4670-4678.
- Umland, T. C., Wei, S.-Q., Cragie, R. and Davies, R. (2000). Structural basis of DNA bridging by barrier-to-autointegration factor. *Biochemistry* **39**, 9130-9138.
- Wang, X., Xu, S., Rivolta, C., Li, L. Y., Peng, G. H., Swain, P. K., Sung, C. H., Swaroop, A., Berson, E. L., Dryja, T. P. et al. (2002). Barrier to autointegration factor interacts with the cone-rod homeobox and represses its transactivation function. *J. Biol. Chem.* **277**, 43288-43300.
- Yamashita, M., Yoshikuni, M., Hirai, T., Fukuda, S. and Nagahama, Y. (1991). A monoclonal antibody against the PSTAIR sequence of p34<sup>cdc2</sup>, catalytic subunit of maturation-promoting factor and key regulator of the cell cycle. *Dev. Growth Differ.* **33**, 617-624.
- Zheng, R., Ghirlando, R., Lee, M. S., Mizuchi, K., Krause, M. and Cragie, R. (2000). Barrier-to-autointegration factor (BAF) bridges DNA in a discrete, higher-order nucleoprotein complex. *Proc. Natl. Acad. Sci. USA* **97**, 8997-9002.